A Genuine GLCM-based Feature Extraction for Breast Tissue Classification on Mammograms

İdil Işıklı Esener*[1], Semih Ergin[2], Tolga Yüksel[1]

Abstract: A breast tissue type detection system is designed, and verified on a publicly available mammogram dataset constructed by the Mammographic Image Analysis Society (MIAS) in this paper. This database consists of three fundamental breast tissue types that are fatty, fatty-glandular, and dense-glandular. At the pre-processing stage of the designed detection system, median filtering and morphological operations are applied for noise reduction and artifact suppression, respectively; then a pectoral muscle removal operation follows by using a region growing algorithm. Then, 88-dimensional texture features are computed from the GLCMs (Gray-Level Co-Occurrence Matrices) of mammogram images. Besides, a formerly introduced 108-dimensional feature ensemble is also computed and cascaded with the 88-dimensional texture features. Finally, a classification process is realized using Fisher's Linear Discriminant Analysis (FLDA) classifier in four different classification cases: one-stage classification, first fatty – then others, first fatty-glandular – then others, and first dense-glandular – then others. A maximum of 72.93% classification accuracy is achieved using only texture features whereas it is increased to 82.48% when cascade features are utilized. This consequence clearly exposes that the cascade features are more representative than texture features. The maximum classification accuracy is attained when "first fatty-glandular – then others" classification case is implemented, that is consistent with the fact that fatty-glandular tissue type is easily confused with fatty and dense-glandular tissue types.

Keywords: Breast tissue, Digital mammography, Feature extraction, Computer-aided detection.

1. Introduction

Breast cancer is the second major cause of female deaths all over the world (Jemal et al; 2011). Although early diagnosis helps mortality to reduce, suspicious mass detection from mammograms becomes harder as breast tissue type becomes denser. Hence, it will be efficient to use a Computer-Aided Detection (CAD) system which can first define the breast tissue type of a mammogram, then detect and diagnose the type of breast cancer. Basically three major problems occur during breast tissue type classification: digitization noise, artifacts like labels of the mammograms, and pectoral muscle regions in the images. Since digitization noise appears as a high-frequency component in an image, smoothing filter implementation such as mean and median filtering is needed for noise reduction (L.M. Mina and N.A.M. Isa, 2014). Besides, histogram processing operations (L.M. Mina and N.A.M. Isa, 2014), curvelet transform (Saha et al; 2015), wavelet transform (Rodigues de Oliveira et al; 2015), and top-hat transform (C. Oral and H. Sezgin, 2013) are commonly used noise reduction methods in the literature.

Another problem is the formation of unwanted artifacts like right/left breast or Craniocaudal (CC)/Mediolateral-Oblique (MLO) shooting labels in the background. This problem is generally handled by the separation of the breast parenchyma from the background applying morphological operations

(L.M. Mina and N.A.M. Isa, 2014), thresholding (Bick et al; 1995), using gradients (Mendez et al; 1996), and active contours (M.A. Wirth and A. Stapinski, 2003).

Almost the most important intensity-based problem for breast tissue classification is the existence of pectoral muscles on the mammogram images. Pectoral muscles show up like triangle geometry at any of the top corners on the mammogram having brighter intensities than breast parenchyma. The studies on pectoral muscle removal in the literature generally focus on intensity-based and wavelet-based approaches. These approaches are examined under three main topics, which are line detection techniques, statistical techniques, and other techniques (Ganesan et al; 2013). Intensity-based approaches either use directly pixel intensities (Saltanat et al; 2010, D.Y.Roshann and K. Harada, 2007, Nagi et al; 2010, Liu et al; 2010, Liu et al; 2012), histogram (K. Thangavel and M. Karnan, 2005; David et al; 2005, Subashini et al; 2010) and gradient (J. Chackraborty and S. Mukhopadhyay, 2012) information of mammogram images or are directly applied to the image gradients (Camilus et al; 2011).

Recent studies on breast tissue type classification mainly performed by Scale Invariant Feature Transforms (SIFT) descriptors (Liasis et al; 2012, S. Kutluk and B. Günsel, 2013, Wang et al; 2011, Bosch et al; 2006) and texton histograms (Liasis et al; 2012, Wang et al; 2011, Chen et al; 2011). In addition to them, local features obtained from Local Binary Pattern (LBP) (Liasis et al; 2012, Chen et al; 2011), Haralick texture descriptors (K. Vaidehi and T.S. Suabshini, 2015, Mustra et al; 2010), Soh features (Mustra et al; 2010), visual word histograms (Diamant et al; 2012), and histogram moments (Liu et

[1] *Department of EEE, Bilecik Seyh Edebali University, Bilecik, Turkey*
[2] *Department of EEE, Eskisehir Osmangazi University, Eskisehir, Turkey*
* *Corresponding Author: Email: idil.isikli@bilecik.edu.tr*

al; 2010, Liu et al; 2011) are other well-known techniques used for breast tissue type classification.

In this paper, the design of a CAD system for breast tissue type classification of mammogram images is aimed. In accordance with this purpose, noise reduction and artifact suppression are initially realized on mammogram images in the database using median filter and morphological operations, respectively. Then, a pectoral muscle removal process is executed using region growing algorithm. These pre-processing operations are elaborately explained in Section 2. A feature extraction procedure explained in Section 3 is performed on the pre-processed mammogram images. The experimental study employed in this paper and all conclusions are given in Sections 4 and 5, respectively.

2. Pre-Processing

Digitization noise, low/high-level artifacts in the background and presence of pectoral muscles, as shown on the sample mammogram image in (Figure.1), obstruct intensity-based breast tissue type classification of mammogram images. Hence, a pre-processing stage is essential in order to reduce noise, suppress artifacts, and remove pectoral muscles on original mammogram images.
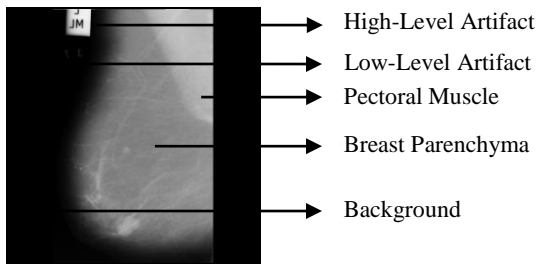

High-Level Artifact

Low-Level Artifact

Pectoral Muscle

Breast Parenchyma

Background

Figure1. Sample mammogram image

2.1. Noise Reduction

Smoothing filters are used for noise reduction although they cause loss in gross details in an image. Hence, the use of filters that can remove noise as well as preserving edge details is essential. In this paper, noise reduction is carried out via median filtering. The median filter is a commonly preferred non-linear filter for noise reduction (Neal et al; 1981). This filter is capable of preserving edge information while removing differences between pixels in the pre-defined neighbourhood.

2.2. Artifact Suppression

Morphological operations are applied for both low and high-level artifact suppressions after noise reduction step. In this respect, the mammography images are converted into their corresponding binary level images. Then, the largest area is assumed to be breast parenchyma on each binary level image since its area should be greater than the area occupied by an artifact.

2.3. Pectoral Muscle Removal

Region growing algorithm is performed for pectoral muscle removal process in this study. Region growing algorithm, a region-based segmentation method, splits all pixels in an image directly into sub-regions by taking the pre-defined similarity conditions for the growing process into consideration (R.C. Gonzalez and R.E. Woods, 2007). This algorithm is based on an enlargement of regions by aggregating the pixels with similar properties. For this purpose, initially, a similarity condition and a seed point or a set of seed points are defined. Specified seed/seed

set is considered as the initial sub-region and the pixels around 4 or 8-neighbors of each pixel are considered in terms of similarity condition.

3. Feature Extraction

3.1. Gray-Level Co-Occurence Matrix (GLCM)

GLCM is one of the commonly used methods for texture analysis and it compares the gray-level differences of any two neighbour pixels in a specified displacement and direction on an image (A. Eleyan and H. Demirel, 2014). In other words, GLCM of an image comprises of a function of the angular relationship and a distance between pixels in the neighbourhood (A. Çalışkan and B. Ergen, 2011). The GLCM of an image I, of size NxN, is formulized in (Equation.1):

$$p(i,j) = \sum_{i=1}^{N} \sum_{j=1}^{N} \begin{cases} 1, & I(x,y)=i \text{ and } I(x+\Delta_x, y+\Delta_y)=j \\ 0, & \text{otherwise} \end{cases} \quad (1)$$

$p(i,j)$ in (Equation.1) refers to the joint probability of co-occurrence of intensities i and j at a given offset (Δ_x, Δ_y) where x and y are the spatial positions in the image. The offset (Δ_x, Δ_y) specifies the distance d and the angle θ between the pixels $I(x,y)$ and its neighborhood.

3.2. GLCM Texture Features

Texture features, introduced by Haralick et al. (Haralick et al; 1973), Soh et al. (Soh and Tsatsaulis, 1999), and Clausi (Clausi, 2002), are extracted from the GLCMs of mammograms in this paper. These features and their mathematical representations are given in (Table.1).

Table 1. GLCM texture features

Feature No	GLCM Texture Features	
	Feature Name	**Mathematical Representation**
	$p(i,j):GLCM = \begin{pmatrix} p(1,1) & \cdots & p(1,N_g) \\ \vdots & \ddots & \vdots \\ p(N_g,1) & \cdots & p(N_g,N_g) \end{pmatrix}$	
	$p_x(i) = \sum_{i=1}^{N_g} p(i,j) \quad , \quad p_y(i) = \sum_{j=1}^{N_g} p(i,j)$	
	$p_{x+y}(k) = \sum_{i=1}^{N_g}\sum_{j=1}^{N_g} p_{i+j=k}(i,j), \quad k=2,3,\cdots,2N_g$	
	$p_{x-y}(k) = \sum_{i=1}^{N_g}\sum_{j=1}^{N_g} p_{|i-j|=k}(i,j), \quad k=0,1,\cdots,N_g-1$	
	$\mu_x = \sum_i \sum_j i\, p(i,j) \quad , \quad \mu_y = \sum_i \sum_j j\, p(i,j)$	
	$\sigma_x = \sum_i \sum_j (i-\mu_x)^2\, p(i,j) \quad , \quad \sigma_y = \sum_i \sum_j (i-\mu_y)^2\, p(i,j)$	
f1	Autocorrelation (Soh and Tsatsaulis, 1999)	$\sum_i \sum_j (i\ j)p(i,j)$
f2	Contrast (Haralick et al; 1973, Soh and Tsatsaulis, 1999)	$\sum_{n=0}^{N_g-1} n^2 \sum_{\substack{i=1 \\ |i-j|=n}}^{N_g}\sum_{j=1}^{N_g} p(i,j)$

Feature No	GLCM Texture Features	
	Feature Name	Mathematical Representation
f3	Correlation (MATLAB)	$$\dfrac{\sum_i \sum_j (i-\mu_x)\cdot(j-\mu_y)\cdot p(i,j)}{\sigma_x \cdot \sigma_y}$$
f4	Correlation (Haralick et al; 1973, Soh and Tsatsaulis, 1999)	$$\dfrac{\sum_i \sum_j (i\ \ j)\ \ p(i,j) - \mu_x\ \ \mu_y}{\sigma_x\ \ \sigma_y}$$
f5	Cluster Prominence (Soh and Tsatsaulis, 1999)	$$\sum_{i=0}^{N_g-1}\sum_{j=0}^{N_g-1}\{i+j-\mu_x-\mu_y\}^4 \cdot p(i,j)$$
f6	Cluster Shade (Soh and Tsatsaulis, 1999)	$$\sum_{i=0}^{N_g\ 1}\sum_{j=0}^{N_g\ 1}\{i+j\ \ \mu_x\ \ \mu_y\}^3\ \ p(i,j)$$
f7	Dissimilarity (Soh and Tsatsaulis, 1999)	$$\sum_i \sum_j |i-j|\cdot p(i,j)$$
f8	Energy (Haralick et al; 1973, Soh and Tsatsaulis, 1999)	$$\sum_i \sum_j \{p(i,j)\}^2$$
f9	Entropy (Soh and Tsatsaulis, 1999)	$$-\sum_{i=0}^{N_g-1}\sum_{j=0}^{N_g-1} p(i,j)\cdot \log\{p(i,j)\}$$
f10	Homogeneity (MATLAB)	$$\sum_i \sum_j \frac{1}{1+|i-j|}\ \ p(i,j)$$
f11	Homogeneity (Soh and Tsatsaulis, 1999)	$$\sum_i \sum_j \frac{1}{1+(i-j)^2}\cdot p(i,j)$$
f12	Maximum Probability (Soh and Tsatsaulis, 1999)	$$\max_{i,j} p(i,j)$$
f13	Sum of Squares: Variance (Haralick et al; 1973)	$$\sum_i \sum_j (i-\mu)^2 \cdot p(i,j)$$
f14	Sum Average (Haralick et al; 1973)	$$\sum_{i=2}^{2N_g} i\cdot p_{x+y}(i)$$
f15	Sum Variance (Haralick et al; 1973)	$$\sum_{i=2}^{2N_g} (i-f_{16})^2 \cdot p_{x+y}(i)$$
f16	Sum Entropy (Haralick et al; 1973)	$$-\sum_{i=2}^{2N_g} p_{x+y}(i)\cdot \log\{p_{x+y}(i)\}$$
f17	Difference Variance (Haralick et al; 1973)	variance of p_{x-y}
f18	Difference Entropy (Haralick et al; 1973)	$$-\sum_{i=0}^{N_g-1} p_{x-y}(i)\cdot \log\{p_{x-y}(i)\}$$
f19	Information Measure of Correlation1 (Haralick et al; 1973)	$\dfrac{HXY-HXY1}{\max\{HX;HY\}}$ $HXY = -\sum_i \sum_j p(i,j)\cdot \log(p(i,j))$ $HXY1 = -\sum_i \sum_j p(i,j)\cdot \log\{p_x(i)\cdot p_y(j)\}$ HX and HY are entropies of p_x and p_y
f20	Information Measure of Correlation2 (Haralick et al; 1973)	$(1-\exp[-2\cdot(HXY2-HXY)])^{1/2}$ $HXY2 = -\sum_i \sum_j p_x(i)\cdot p_y(j)\cdot \log\{p_x(i)\cdot p_y(j)\}$
f21	Inverse Difference Normalized (Clausi, 2002)	Normalized Homogeneity (MATLAB)
f22	Inverse Difference Moment Normalized (Clausi, 2002)	Normalized Homogeneity (Soh and Tsatsaulis, 1999)

Texture features, extracted in this paper, give information about the homogeneity, symmetry, complexity, and contrast in the GLCMs of the mammogram images.

4. Experimental Study

In this paper, a CAD system that classifies mammogram images into the breast tissue types of fatty, fatty-glandular, and dense-glandular is proposed. Firstly, a pre-processing of mammogram images is performed where median filtering and morphological operations are applied for noise reduction and artifact suppression, respectively; then a pectoral muscle removal process follows by using region growing algorithm. Secondly, at the feature extraction stage, 88-dimensional texture features are computed from the GLCMs of mammogram images. Finally, classification is realized using Fisher's Linear Discriminant Analysis (FLDA) in four different classification cases.

4.1. Database

A publicly available mammogram database constructed by the Mammographic Image Analysis Society (MIAS) is used in this paper (Suckling et al; 1994). This database consists of three health status classes (normal, benign, malignant) for each of three breast tissue type classes (fatty, fatty-glandular, and dense-glandular). It has 322 MLO mammogram images (106 fatty, 104 fatty-glandular, and 112 dense-glandular) with 330 diagnosis (207 normal, 69 benign, and 54 malignant). The images in the MIAS database are of size 1024x1024 at 200 μm/pixel resolution and they are in ".pgm" imaging format.

All mammogram images in the database are resized into a size of 256x256 for ease of operation. Sample images of each class in the MIAS database are shown in (Figure.2). The rows and columns in the (Figure.2) show three different samples of health status and breast tissue types.
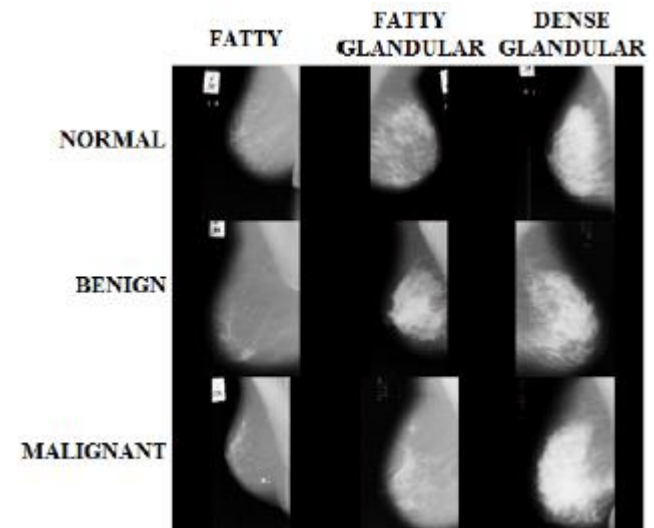

Figure2. Sample mammogram images in the MIAS database

4.2. Feature Vector Construction

In this paper, the texture features, given in (Table.1), are computed from the GLCMs of the mammogram images.
The GLCMs of mammogram images are obtained in four different rotation directions which has an angle of $\Theta = 0°$, 45°, 90°, and 135° using four different pixel distances $d =\{1, 2, 3, 4\}$. Hence, four co-occurrence matrices are evaluated for each rotation direction, and 22-dimensional textural

Table 2. The classification accuracies obtained using only texture features

Classification Case	Classification Accuracies (%)				
	1. Fold	2. Fold	3. Fold	4. Fold	Average
1-Stage Classification	66.23	46.75	62.34	66.23	60.39
"First Fatty – Then Others" Classification	70.42	62.32	75.53	67.12	68.35
"First Fatty-Glandular – Then Others" Classification	77.78	72.55	70.18	71.21	72.93
"First Dense-Glandular – Then Others" Classification	69.01	50.72	66.67	71.01	64.35

feature vectors are computed from each of co-occurrence matrices. Then, the average of these four matrices is calculated so that a 22-dimensional feature vector is constructed for the corresponding direction. Ultimately, 88-dimensional feature vectors for each mammogram image are obtained by concatenating four different 22-dimensional feature vectors of each direction.

4.3. Classification

Breast tissue type classification is performed in one-stage and two-stage processes in this paper. In the one-stage classification process, mammogram images are directly categorized as having fatty, fatty-glandular, and dense-glandular tissue types. Besides, the two-stage classification process is carried out in three different ways: *first fatty – then others*, *first fatty-glandular – then others*, and *first dense-glandular – then others*.

In the first stage of the "*first fatty – then others*" classification process, the mammogram images are primarily classified as fatty and non-fatty mammograms. Then, in the second stage, the mammograms labeled as non-fatty are classified as fatty-glandular and dense-glandular. Similarly, in the "*first fatty-glandular – then others*" classification case, mammograms are firstly classified as fatty-glandular and non-fatty-glandular, and then non-fatty-glandular mammograms are classified as fatty and dense-glandular. Finally, in the "*first dense-glandular – then others*" classification case, mammograms are initially categorized as dense-glandular and non-dense-glandular, and then non-dense-glandular mammograms are classified as fatty and fatty-glandular.

4.4. Performance Evaluation

In this paper, a breast tissue type detection system is designed for four different classification cases using FLDA classifier. Average and fold-by-fold classification accuracies of FLDA

classifier when texture features are used in four classification processes are given in (Table.2). The maximum average classification accuracy of 72.93% is achieved when "*first fatty-glandular – then others*" classification case is implemented.

In addition to the GLCM texture features, the 108-dimensional feature ensemble introduced in (Işıklı Esener et al; 2015) is computed in order to increase the data representability of the existent GLCM features. This 108-dimensional feature ensemble is formed as the concatenation of some statistical and frequency domain features to the LCP-based feature vectors (Işıklı Esener et al; 2015). Then, the 88-dimensional texture features and the 108-dimensional feature vectors are spliced. Consequently, 196-dimensional feature vectors are obtained for each mammogram image. Average and fold-by-fold classification accuracies are given in (Table.3) when the spliced 196-dimensional features are used. The maximum average classification accuracy is increased to 82.48% when spliced features are used instead of only textural features. This rise in classification accuracy proves that the feature ensemble (Işıklı Esener et al; 2015) strengthens the data representability of GLCM texture features. Moreover, the maximum average classification accuracy is again attained in "*first fatty-glandular – then others*" classification cases. The maximum classification accuracy is reached when "*first fatty-glandular – then others*" classification case is performed. It is already known by radiologists that fatty-glandular tissues can easily be confused with fatty and dense-glandular tissue types. Hence, it would be wisely to detect fatty-glandular tissue type primarily, and then re-categorize non-fatty-glandular ones as fatty or dense-glandular. This reality is quite coherent with the classification process that gives maximum classification accuracy.

Table 3. The classification accuracies obtained using 196-dimensional feature vectors

Classification Case	Classification Accuracies (%)				
	1. Fold	2. Fold	3. Fold	4. Fold	Average
1-Stage Classification	72.73	55.84	77.92	53.25	64.94
"First Fatty – Then Others" Classification	78.57	57.97	87.30	65.71	72.39
"First Fatty-Glandular – Then Others" Classification	89.29	77.78	84.85	78.00	82.48
"First Dense-Glandular – Then Others" Classification	80.00	62.12	81.54	77.42	75.27

5. Conclusion

In this paper, a Computer Aided Detection (CAD) system for breast tissue type classification is designed, and it is verified on a popular mammogram database compiled by the Mammographic Image Analysis Society (MIAS). This database consists of the mammograms of three fundamental breast tissue types namely fatty, fatty-glandular, and dense-glandular. The 88-dimensional texture features computed from GLCMs of the mammogram images, are concatenated to the 108-dimensional feature ensemble. Ultimately, 196-dimensional feature vectors are obtained for each mammogram image and then they are classified using Fisher's Linear Discriminant Analysis (FLDA) classifier in four different classification cases: one-stage classification, first fatty – then others, first fatty-glandular – then others, and first dense-glandular – then others.

A maximum of 72.93% classification accuracy is achieved using only texture features while it is increased to 82.48% when the final 196-dimensional feature vectors are employed. This consequence clearly implies that the final concatenated feature vectors are more descriptive than texture features. Besides this finding, the increase in the number of the dimension for the evaluated feature vectors reveals more representative vectors so that mammogram images are eventually characterized more effectively.

References

[1] A. Jemal, F. Bray, M. M. Center, J. Ferlay, E. Ward and D. Forman (2011). Global cancer statistics. CA: A Cancer Journal for Clinicians. Vol. 61. No.2. Pages. 69-90.

[2] L. M. Mina and N. A. M. Isa (2014). Preprocessing technique for mammographic images. International Journal of Computer Science and Information Technology Research. Vol. 2. Pages. 226-231.

[3] M. Saha, M. K. Naskar and B. N. Chatterji (2015). Mammogram denoising by curvelet transform based on the information of neighbouring coefficients. Third IEEE International Conference on Computer, Communication, Control and Information Technology (C3IT), Hooghly, Inda. Pages. 1-6.

[4] H. C. Rodigues de Oliveira, L. Rodrigues Borges, P. Ferreira Nunes, P. R. Bakic, A. D. A. Maidment and M. A. C. Vieira (2015). Use of wavelet multiresolution analysis to reduce radiation dose in digital mammography. 28th IEEE International Symposium on Computer-Based Medical Systems (CBMS), São Carlos and Ribeirão Preto, Brazil. Pages. 33-37.

[5] C. Oral and H. Sezgin (2013). Effects of dimension reduction in mammograms classification. Eighth International Conference on Electrical and Electronics Engineering (ELECO), Bursa, Turkey. Pages. 630-633.

[6] U. Bick, M.L. Giger, R. A. Schmidt, R. M. Nishikawa, D. E. Wolvertan and K. Doi (1995). Automated segmentation of digitized mammograms. Academic Radiology, Vol. 2. No. 2. Pages. 1-9.

[7] A. J. Mendez, P. J. Tahaces, M. J. Lado, M. Souto, J. L. Correa and J. J. Vidal (1996). Automatic detection of breast border and nipple in digital mammograms. Computer Methods and Programs in Biomedicine. Vol.

[8] M. A. Wirth and A. Stapinski (2003). Segmentation of the breast region in mammograms using active contours. Viusal Communications and Image Processing (VCIP), Lugano, Switzerland. Pages. 1995-2006.

[9] K. Ganesan, U. R. Acharya, K. C. Chua, L. C. Min and K. T. Abraham (2013). Pectoral muscle segmentation: A review. Computer Methods and Programs in Biomedicine. Vol. 110. Pages. 48-57.

[10] M. Saltanat, M. A. Hossain and M. S. Alam (2010). An efficient pixel value based mapping scheme to delineate pectoral muscle from mammograms. Fifth IEEE International Conference on Bio-Inspired Computing: Theories and Applications (BIC-TA), Changsha, China. Pages. 1510-1517.

[11] D. Y. Roshann and K. Harada (2007). A connected component labelling algorithm for grayscale images and application of the algorithm on mammograms. The 22nd Annual ACM Symposium on Applied Computing (SAC), Seoul, Korea. Pages. 146-152.

[12] J. Nagi, S. A. Kareem, F. Nagi and S. K. Ahmed (2010). Automated breast profile segmentation for ROI detection using digital mammograms. IEEE EMBS Conference on Biomedical Engineering & Sciences (IECBES), Kuala Lumpur, Malaysia. Pages. 87-92.

[13] L. Liu, J. Wang, and K. He, "Breast density classification using histogram moments of multiple resolution histograms", In: 3rd International Conference on Biomedical Engineering and Informatics, pp. 146-149, 2010.

[14] C. C. Liu, C. Y. Tsai, J. Liu, C. Y. Yu, and S. S. Yu, "A pectoral muscle segmentation algorithm for digital mammograms using Otsu thresholding and multiple regression analysis", Computers & Mathematics with Applications, vol. 64, no. 5, pp. 1100-1107, 2012.

[15] K. Thangavel and M. Karnan, "Computer aided diagnosis in digital mammograms: Detection of microcalcifications by meta heuristic algorithms", International Journal on Artificial Intelligence and Machine Learning, vol. 5, pp. 29-40, 2005.

[16] R. David, O. Arnau, M. Joan, P. Marta and E. Joan (2005). Breast segmentation with pectoral muscle suppression on digital mammograms. Lecture Notes in Computer Science. Pages. 153-158.

[17] T. S. Subashini, V. Ramalingam and S. Palanivel (2010). Pectoral muscle remocal and detection of masses in digital mammogram using CCL. International Journal of Computer Applications. Vol.1. No. 6. Pages. 71-76.

[18] J. Chakraborty and S. Mukhopadhyay (2012). Automatic detection of pectoral muscle using average gradient and shape based feature. Journal of Digital Imaging. Vol. 25. Pages. 387-399.

[19] K. S. Camilus, V. K. Govindan and P. S. Sathidevi (2011). Pectoral muscle identification in mammograms", Journal of Applied Clinical Medical Physics. Vol. 12. No. 3. Pages. 215-230.

[20] G. Liasis, C. Pattichis and S. Petroudi (2012). Combination of different texture features for mammographic breast density classification. 12th IEEE International Conference on Bioinformatics & Engineering (BIBE), Nicosia, Cyprus, Pages. 732-737.

[21] S. Kutluk and B. Günsel (2013). Tissue density classification in mammographic images using local

features. 21st Signal Processing and Communications Applications Conference (SIU), Haspolat-Nikosia, North Cyprus. Pages. 1-4.

[22] J. Wang, Y. Li, Y. Zhang, H. Xie and C. Wang (2011). Bag-of-features based classification of breast parenchymal tissue in the mammogram via jointly selecting and weighting visual words. 6th IEEE International Conference on Image and Graphics (ICGIP), Tokyo, Japan. Pages: 622-627.

[23] A. Bosch, X. Munoz, A. Oliver and J. Marti (2006). Modeling and classifying breast tissue density in mammograms. IEEE Computer Society Conference on Computer Vision and Pattern Recognition (CVPR), Las Vegas, Nevada. Pages. 1552-1558.

[24] Z. Chen, E. Denton and R. Zwiggelaar (2011). Local feature based mammographic tissue pattern modelling and breast density classification. 4th IEEE International Conference on Biomedical Engineering and Informatics (BMEI), Shanghai, China, Pages. 351-355.

[25] K. Vaidehi and T.S. Subashini (2015). Automatic classification and retrieval of mammographic tissue density using texture features. 9th IEEE International Conference on Intelligent Systems and Control (ISCO), Coimbatore, India, Pages. 1-6.

[26] M. Mustra, M. Grgic and K. Delac (2010). Feature selection for automatic breast density classification. 52nd IEEE International Symposium ELMAR (ELMAR), Zadar, Crotia. Pages. 9-16.

[27] I. Diamant, H. Greenspan and J. Goldberger (2012). Breast tissue classification in mammograms using visual words. 27th IEEE Convention of Electrical & Electrronics Engineers in Israel (IEEEI), Eilat, Israel. Pages. 1-4.

[28] L. Liu, J. Wang and K. He (2010). Breast density classification using histogram moments of multiple resolution mammograms. Third IEEE International Conference on Biomedical Engineering and Informatics (BMEI), Yantai, China. Pages. 146-149.

[29] Q. Liu, L. Liu, Y. Jan, J. Wang, X. Ma and H. Ni (2011). Mammogram density estimation using sub-region classification. Fourth IEEE International Conference on Biomedical Engineering and Informatics (BMEI), Shanghai, China. Pages. 356-359.

[30] C. Neal, Jr. Gallagher and G.L. Wise (1981). A theoretical analysis of the properties of median filters: IEEE Transactions on Acoustics, Speech, and Signal Processing. Vol. ASSP-29. No. 6. Pages. 1136-1141.

[31] R. C. Gonzalez and R. E. Woods (2007). Digital Image Processing. 3. Ed.

[32] A. Eleyan and H. Demirel (2011). Co-occurrence matrix and its statistical features as a new approach for face recognition. Turkish Journal of Electrical Engineering & Computer Sciences. Vol. 19. No. 1. Pages. 97-107.

[33] A. Çalışkan and B. Ergen (2014). Palmprint Recognition System based on Gray Level Co-Occurrence Matrix. 22nd Signal Processing and Communications Applications Conference (SIU), Trabzon, Turkey. Pages. 826-829.

[34] R. M. Haralick, K. Shanmugam and I. Dinstein (1973). Textural features of image classification. IEEE Transactions on Systems, Man and Cybernetics. Vol. SMC-3, No. 6.

[35] L. Soh and C. Tsatsaulis (1999). Texture analysis of SAR sea ice imagery using gray level co-occurrence matrices. IEEE Transactions on Geoscience and Remote Sensing. Vol. 37. No. 2.

[36] D. A. Clausi (2002). An analysis of co-occurrence texture statistics as a function of grey level quantization. Can. J. Remote Sensing. Vol. 28. No. 1. Pages. 45-62.

[37] J Suckling et al. (1994). The Mammographic Image Analysis Society Digital Mammogram Database. Exerpta Medica. International Congress Series 1069. Pages. 375-378.

[38] I. I. Esener, S. Ergin and T. Yüksel (2015). A new ensemble of features for breast cancer diagnosis. 38th IEEE International Convention on Information and Communication Technology, Electronics and Microelectronics (MIPRO), Opatija, Crotia. Pages. 1168-1173.